Hindawi Publishing Corporation
Journal of Nanomaterials
Volume 2009, Article ID 245941, 10 pages
doi:10.1155/2009/245941

Research Article

Size Dependence of Dislocation-Mediated Plasticity in Ni Single Crystals: Molecular Dynamics Simulations

Xiaoyan Li and Wei Yang

Department of Engineering Mechanics, Tsinghua University, Beijing 100084, China

Correspondence should be addressed to Wei Yang, yw-dem@mail.tsinghua.edu.cn

Received 16 May 2008; Accepted 21 September 2008

Recommended by Yapu Zhao

We investigate the compressive yielding of Ni single crystals by performing atomistic simulations with the sample diameters in the range of 5 nm ~ 40 nm. Remarkable effects of sample sizes on the yield strength are observed in the nanopillars with two different orientations. The deformation mechanisms are characterized by massive dislocation activities within a single slip system and a nanoscale deformation twining in an octal slip system. A dislocation dynamics-based model is proposed to interpret the size and temperature effects in single slip-oriented nanopillars by considering the nucleation of incipient dislocations.

1. Introduction

It has been widely known that the sample size bears significant effects on the mechanical properties of materials. Early researches illustrated that the plastic yielding of microscale whiskers was closely related to the formation of Lüders bands [1, 2]. The theoreticians then claimed that the smaller was stronger [3]. The tension and torsion testing [4] on thin copper wires indicated a distinct dependence of yield strength on sample sizes. Recently, compression experiments on microscale pillars machined by focused-ion-beam demonstrated that the yield strength of single crystals could rise steadily with the decrease of sample diameter [5–7]. These size effects were originated from the microstructural and dimensional constraints [8]. At present, discrete dislocation simulations [9–11] were used to investigate the effect of sample size on strength in the submicron-to-micron range. The relevant results highlighted the interplay between sample size, internal stress, and length scale inherent to dislocation generation and motion [9–11]. For metallic nanowires, both atomistic simulations [12] and experimental observations [13] revealed that the size strengthening was closely associated with a phase transformation induced by surface stress [14]. By scanning tunneling microscope [15, 16], it was found that a single atom chain has or may have extremely strong strength attributed to quantized plasticity [13].

Currently, understanding of size effects of microscale single crystal focuses on the operative mechanisms for crystal plasticity under nominally uniform compression. The dislocation starvation model [6] was proposed to reflect the discrete stain bursts separated by periods of nearly elastic loading. This model elucidates that the rate of dislocation escape from the free surface is greater than that of dislocation multiplication in the small scale crystal. It is suggested that the sample sizes physically limit the free distance that dislocations can travel for breeding and replicating [6]. According to a theoretical analysis concerning the dislocation kinetics, the microscale size effects are attributed to dislocation nucleation, dislocation escape, and dislocation trapping [7]. These stochastic effects alter the distribution of dislocation sources and restrict the multiplication processes, leading to reduction of the dislocation density and finally exhaustion hardening [7]. Based on molecular dynamics (MD) simulations for homogeneous shear of Ni_3Al single crystal, a scaling model involving the statistical distribution of atomic relative displacements was present to predict the size dependence of incipient dislocation plasticity in microscale samples by extrapolation [17]. Furthermore, a survival probability theory [18] of homogeneous dislocation

generation was proposed in the stochastic nature of yield strength of microscale crystals. For the prediction of incipient plasticity behavior, this methodology bridges both the length and time scales between MD and experimental regimes [18]. Combined this statistical methodology, the dislocation nucleation from the free surfaces has been revealed by the analysis of elastic instability [19]. The recent work rationalized the size effects by considering the statistical variation of dislocation source lengths in the finite size single crystals [20]. This work also suggests that the discussions about size effects should be divided into two regimes: one is dislocation nucleation and propagation in very small crystals and the other is operation of exiting dislocation sources for larger microscale crystals. Excitingly, state-of-the-art in situ nanocompression experiments give a clear evidence of dislocation starvation model and further demonstrate that the strength increase in the small pillar structure is controlled by the activation of new dislocation sources in a source-limited regime [21].

In this paper, we carry out molecular dynamics (MD) simulations to investigate the compressive plastic yield of Ni single crystal nanopillars. The compressions of nanopillars with two different orientations provide the observation of distinct deformation mechanisms for single and octal slip behaviors. Furthermore, the influences of finite temperature on yield strength are explored. To account for the dependence of yield strength on sample size and temperature, we present a dislocation mechanics-based model by considering incipient dislocation plasticity.

2. Simulation Method

The simulated configuration is a pillar with a fixed length-to-diameter ratio of 2:1. The diameters of the pillars range from 5 nm to 40 nm. Consequently, the simulated systems contain approximately 18000 to 9000 000 Ni atoms. Referring to a perfect fcc lattice arrangement, we orient the pillars in the directions of [134] (single slip) and [001] (octal slip), respectively, with respect to the compressing axis. Throughout MD simulations, interatomic interactions are described by an embedded atom method (EAM) potential [22]. To improve the efficiency of simulations, we adopt a multiple time step algorithm [23] as the numerical integrator. The shorter and the longer time steps are set to be 0.5 femtosecond (fs) and 1.5 femtoseconds, respectively. By a Gaussian thermostat [24], the temperature of simulation is controlled at the prescribed values from 100 K to 900 K.

At the beginning of all simulations, single crystal pillars were relaxed free for 50 picoseconds (ps) to minimize the potential energy of system. Subsequently, uniaxial compressions were performed on the nanopillars. In each loading step, an incremental compressive displacement of 0.04% in the length direction was imposed on the top face, followed by a dynamic relaxation of 4 picoseconds for the overall pillar. During such process, the side surface was kept free and the bottom face was adhered to the rigid foundation, resembling a clamped end. Atoms in the loading region retained the same plane all along. This loading procedure led to a relatively high-strain rate of $10^8\,s^{-1}$ (inevitable for MD simulations) relative to the experimental strain rates (approximately $10^{-4}\,s^{-1}$ or $4 \times 10^{-3}\,s^{-1}$). The overall simulations last 2 nanoseconds, and, therefore, the maximal strain of simulated system reaches 20%. The local crystalline order analysis [25–27] assisted by coordination number technique was employed to visualize defects appearing in the deformation. Moreover, the stresses of nanopillar were calculated through averaging atomic stresses described by the Virial theorem.

Due to an inherent limitation of MD simulations [28], the high deformation rate applied in simulations may induce rather high stresses which are usually much larger than results of experiments. However, this artificially high rate cannot change the underlying deformation physics in the single crystals. To avoid probing unphysical behavior, the applied stress is verified to lie well below the theoretical shear strength of single crystal in the particular direction of straining [28]. It is also essential that the time scale, on which the simulated behavior occurs (e.g., the velocity of gliding dislocation), is verified to lie well below any critical inherent time scale of single crystal (such as the speed of sound) [28]. Although MD simulations are limited to relatively small systems consisting of typically millions of atoms, such massive simulations represent a promising step toward elucidating the intrinsic mechanisms of size effects for microscale single crystals.

3. Results and Discussion

Figure 1 displays the stress-strain curves of ⟨134⟩- and ⟨001⟩-oriented nanopillars at 300 K. If the maximal stress on the curve is taken as the yield strength, dramatic size effects are observed for Ni single crystals under nominally single slip or octal slip conditions. As illustrated in Figure 1, the flow stress drops to a low level after yielding. Such a phenomenon differs from the experimental observations in which the flow stress maintains at the level of yield strength [5–7]. One interpretation comes from the initially defect-free status of the nanopillars before compression. The similar stress drop also occurred in the atomistic simulations for nanowires [12, 29] and single crystal blocks [30]. The high-frequency stress oscillations are attenuated as the size increases, as evidenced in Figure 1. This indicates that the local atomic vibrations play a critical role at the scale below 20 nm. These local effects are weakened by size increasing due to a global stress averaging procedure [30]. Figure 2 shows the variation of activation volume with the diameter of ⟨134⟩-oriented nanopillars. For the small size nanopillars, the present activation volume is consistent with the result from a recent atomistic modelling about surface dislocation nucleation [31]. Herein, the activation volume is obtained by totalizing the Virial volumes of atoms in the nucleated dislocation at the first stress drop. The present activation volumes are atomic rather than the volume expected from an actual dislocation [32]. The rise of activation volume with an increase of sample size implies that the dislocation generation corresponding to initial yielding appears to follow homogeneous nucleation kinetics [17].

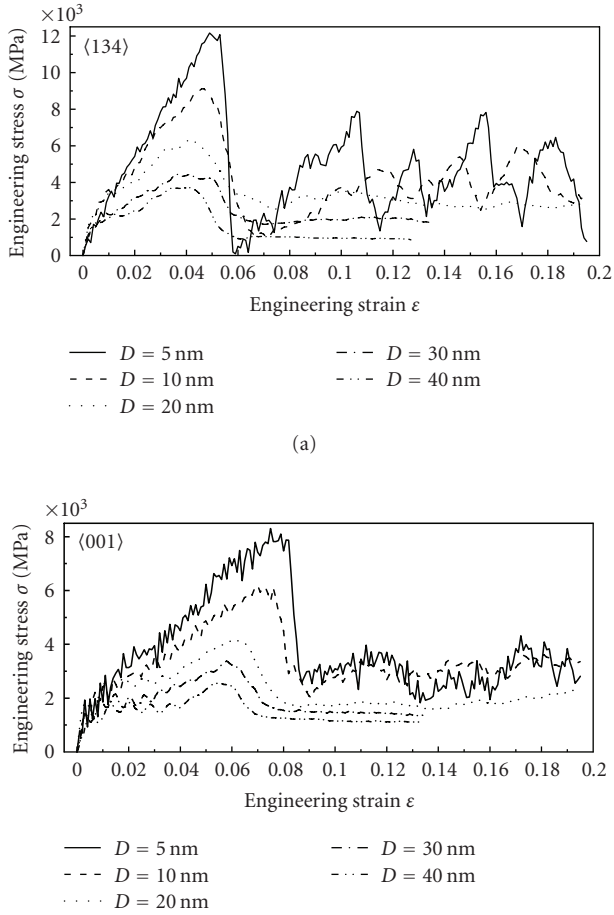

FIGURE 1: Stress-strain curves of ⟨134⟩- and ⟨001⟩-oriented nanopillars at 300 K.

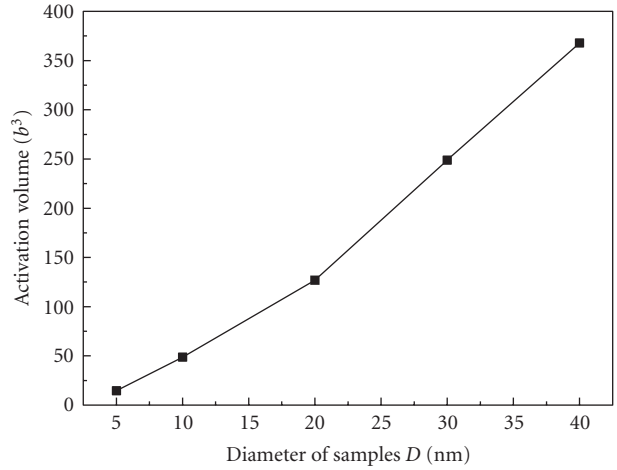

FIGURE 2: Variation of activation volume with the diameter of ⟨134⟩-oriented at 300 K. The sign "b" represents the magnitude of Burgers vector of extended dislocation.

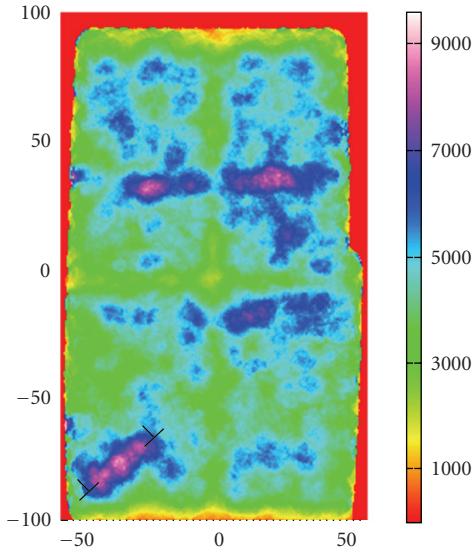

FIGURE 3: Octahedral shear stress distribution at initial yielding of 10 nm ⟨134⟩-oriented nanopillar. The stress value of each point is obtained by averaging the Virial stresses of atoms in a sphere (centered at this point and with a radius of the cut-off distance used in the EAM potentials). The length unit is Angstrom, and the stress unit is MPa.

For the pillars less than 20 nm in diameter, their stress-strain curves are featured by several sharp fluctuations that correspond to the discrete nucleation of dislocations. To reveal dislocation nucleation events, Figure 3 depicts an image of octahedral shear-stress distribution at initial yielding of 10 nm ⟨134⟩-oriented pillar. This stress distribution exhibits dynamical propagation of stress waves, distinctly unlike the quasistatic stress states reported in the literature [7]. In all of simulations, an instantaneous stress drop-off concurred with dislocation emission from the corners or the free surfaces, implying that the stress drop-off after yielding is indicative to the onset of incipient dislocation plasticity [17]. In addition, Figures 4(a)–4(c) display the stress-strain relations of nanopillars at different temperatures. As shown in Figure 4, the yield strength of nanopillars decreases with an increase of temperature. It suggests that temperature is a significant external factor for the occurrence of initial yielding of nanopillars because the incipient dislocation nucleation is a thermally activated event [17]. Meanwhile, the stress oscillations become more and more prominent in the stress-strain curves with an increase of temperature since the atomic vibrations are gradually quickened. Moreover, the curves shown in Figure 4 also clearly indicate that the high temperature induces a thermal softening of elastic properties.

Figure 5 depicts the microstructure evolution of 20 nm ⟨134⟩-oriented nanopillars under the compression. The extended dislocation initially nucleates from a corner and then travels through the perfect crystal along a primary glide plane. When reaching the free surface at the opposite end, it is reflected after leaving a tiny surface step. Such process substantiates that the overall sample sizes limit the length scales available for the plasticity process [5]. The reflected dislocation meets with the emitted dislocations located at the

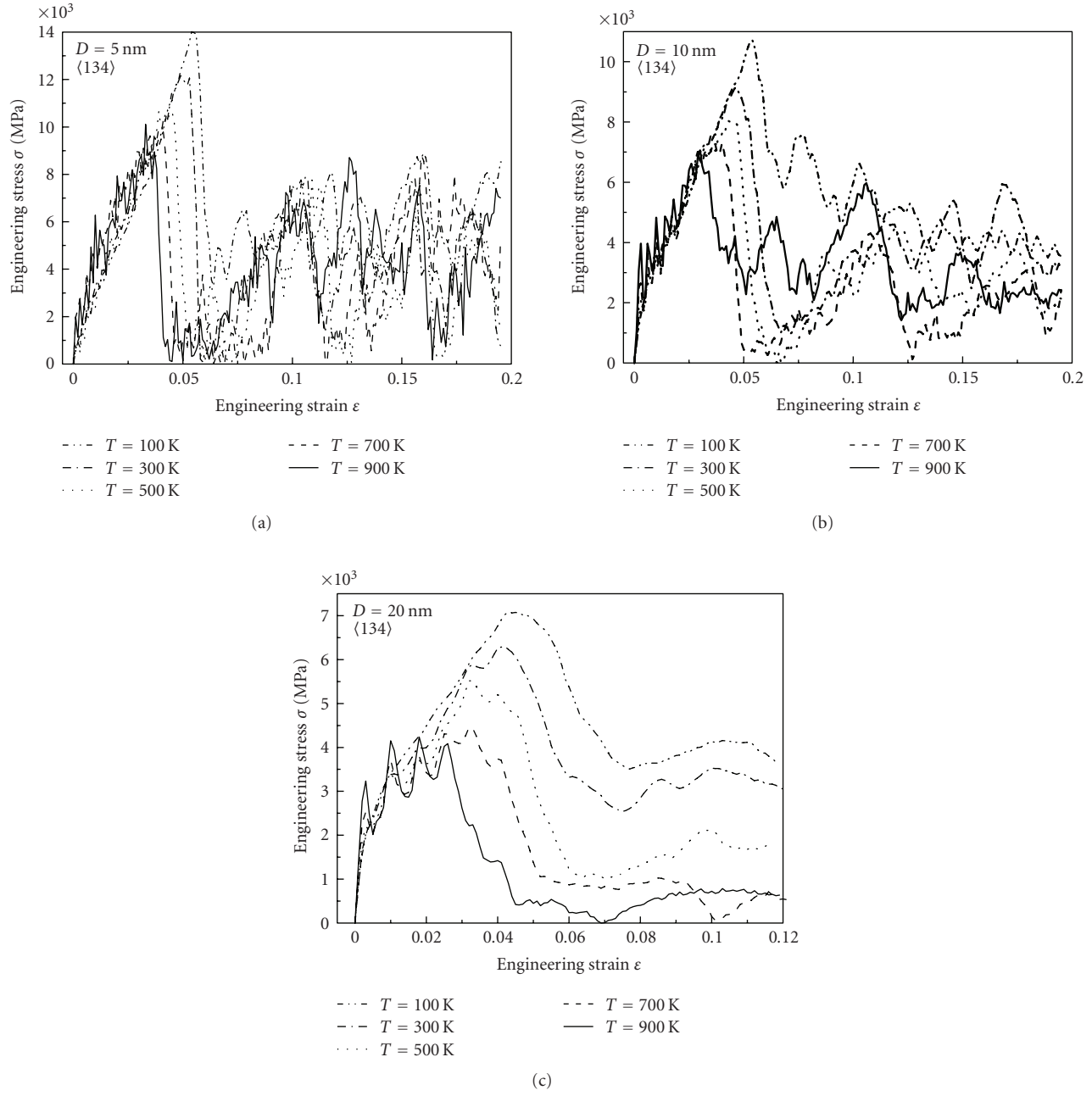

Figure 4: Stress-strain curves of ⟨134⟩-oriented nanopillars at different temperatures.

same slip plane. Then, they either annihilate or react with each other, leading to formation of a few defects, such as vacancy chains and new dislocations. As the compression proceeds, the activation of secondary slip plane results in further dislocation motion, reaction, and even multiplication (even involving double-cross-slip). The successive emissions of dislocations on primary slip system induce a global sliding of the top-left part of nanopillar, as shown in Figure 5(e). This inhomogeneous deformation mode can explain glide offset and lateral displacement of the top portion of single crystal relative to the fixed end [7]. Further developments of single-slip offsets may cause plastic flow involving strain bursts governed by accumulative growth of dense dislocation structures [33].

Figure 6 illustrates the microstructure evolution of 20 nm ⟨001⟩-oriented nanopillars under compression. Several extended dislocations, namely, stack fault (SF) areas towed by partial dislocation, firstly, nucleate from the corners, then, glide on the slip planes of {111}-type, and finally, merge into the free surface with remnant surface steps. Thus, perfect single crystal can be transected by several SFs remaining in the crystal interior, which circumscribes further dislocation motion. The local stress may induce nanoscale twins from the coupled partial dislocations on the neighboring

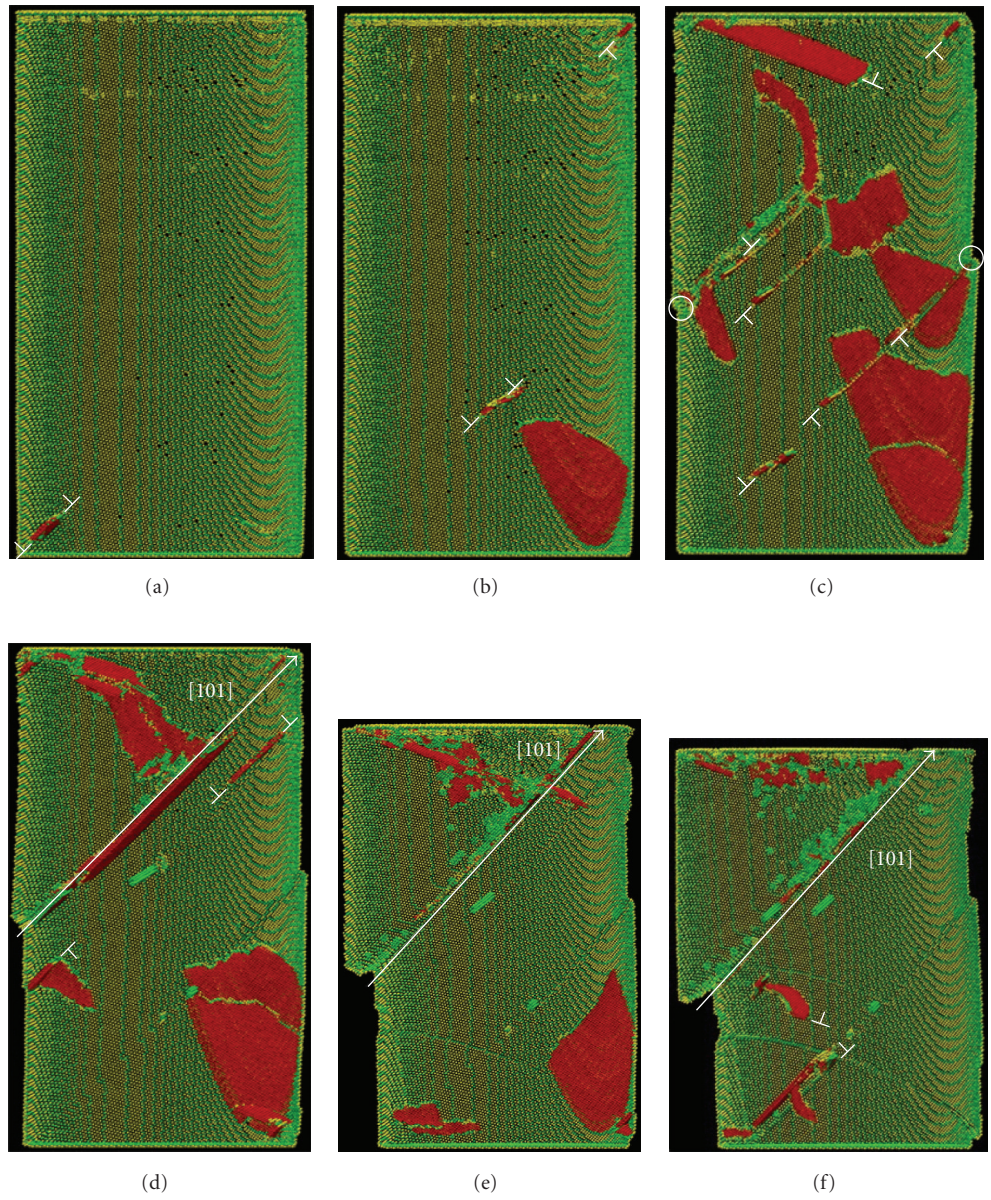

Figure 5: Snapshots for microstructure evolution in 20 nm ⟨134⟩-oriented nano-pillar. (a)–(c) The extended dislocations nucleate, glide and reflect at the free surfaces. (d)–(f) The top-left part of the pillar undergoes global sliding, leading to strain bursts. The symbol "◯" marks the surface step. Slip lines and surface steps are clearly observed in the deformed states.

glide planes. Such small scale twins are determined by dimensionally constrained structures and serve as barriers to further dislocation activities. However, the intersection of twins becomes new defect sources under high-applied stress. The emission and propagation of partial dislocations from the active sources will broaden the twin spacing, which significantly reduces the ductility of nanopillars [34]. When two parallel twin boundaries encounter, the hcp atom layers recover the perfect fcc structures. As a result, two nanoscale twins are incorporated into a new twin.

Figures 5(f) and 6(f) illustrate the final deformation microstructures of ⟨134⟩- and ⟨001⟩-oriented pillars with a diameter of 20 nm, respectively. The appearances of samples after compression are analogous to those in experiments [5–7]. For nanopillars orientated to favor single slip, plastic behaviors are governed by intense dislocation activities including nucleation, propagation, multiplication, and interaction. For nanopillars with the octal-slip orientation, nanoscale twinning is a dominant deformation mechanism controlling plastic flow. The above mechanisms indicate that crystal internal orientation is responsible to the physical nature of irreversible deformation. Nevertheless, two dissimilar mechanisms are consistent in the aspect of underlying physics, since they are strongly governed by dislocation plasticity. All details of microstructure evolution predicted by different deformation mechanisms are expectantly

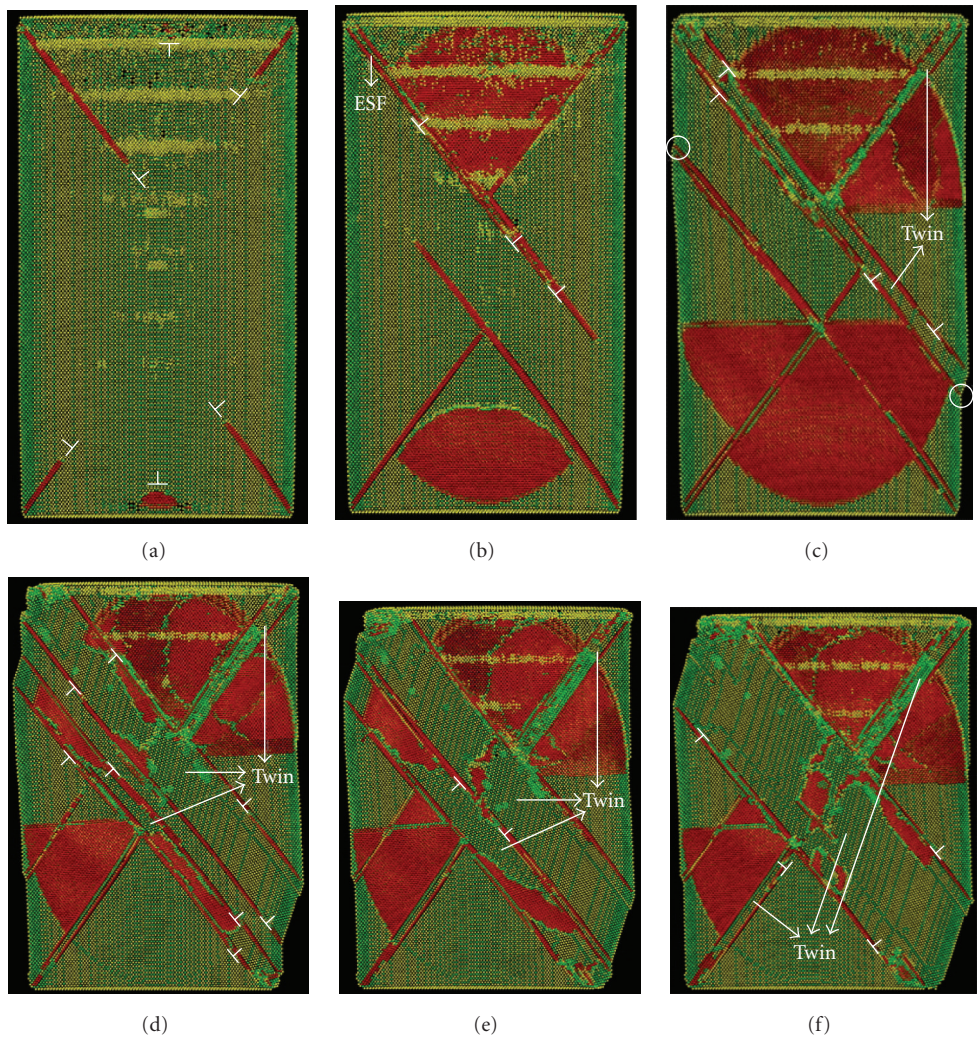

FIGURE 6: Snapshots for microstructure evolution in 20 nm ⟨001⟩-oriented nanopillar. (a) Poly-slip behavior concurs with yielding. (b)-(d) Nanoscale twins are formed and then broaden by the successive emission of Shockley partial dislocations. (e)-(f) Two parallel twin boundaries annihilate as a result of a new nanoscale twin. The symbol "◯" marks the surface step. Slip lines and surface steps are clearly observed in the deformed states.

supported by the transmission electron microscopy (TEM) analysis of experimental samples before and after compression.

To better understand finite size and temperature effects, we develop a dislocation dynamics-based model which is applicable to single-slip behaviors. Based on the thermal activation analysis [35, 36] and intrinsic stress scaling [37], the shear strength τ_S consists of the thermal stress τ_T and the size-related stress τ_D,

$$\tau_S = \tau_T + \tau_D = A_1 \exp\left[-\beta_0 T + \beta_1 T \ln\left(\frac{\dot{\gamma}}{\dot{\gamma}_0}\right)\right] + A_2\left(\frac{D}{D_0}\right)^n, \tag{1}$$

where τ_T represents a threshold value of dislocation nucleation; and τ_D depends on the sample diameter D (normalized by a reference diameter $D_0 = 1\,\mu m$) by a power law of exponent n. In (1), $\dot{\gamma}$ and $\dot{\gamma}_0$ are the actual and the reference shear strain rates; T is the absolute temperature; and parameters A_1, A_2, β_0, and β_1 are constants for a given material under a specific condition. Based on the experimental results [5, 7] and the present MD simulations, we use a nonlinear least-squares fit to determine the related parameters as follows:

$$\begin{aligned} n &= -0.69, \\ A_1 &= 2224.17 \pm 297.56\,\text{MPa}, \\ A_2 &= 124.68 \pm 11.47\,\text{MPa}, \\ \beta_0 &= (12.01 \pm 2.07) \times 10^{-3}\,\text{K}^{-1}, \\ \beta_1 &= (4.40 \pm 0.35) \times 10^{-4}\,\text{K}^{-1}. \end{aligned} \tag{2}$$

These data are optimized values by repeated fit procedure. The exponent n denotes a fractal dimension between the strength and the internal structure [37]. Its value locates in the suggested range of $-0.6 \sim -0.7$ [7].

Yield behaviors in the nearly dislocation-free materials are not dominated by the morphological distribution or assembling density of dislocations, but by the nucleation and propagation of dislocations [30, 31]. During the present simulations for single-slip oriented nanopillars, yielding occurs when the first extended dislocation nucleates from the surface and sweeps through the pillar. Figure 6(a) describes a glide process of the first extended dislocation travelling through the crystals with different diameters. The observed geometries suggest that the curvature radii of the leading and trailing partial dislocations are proportional to the sample diameters, that is, $R_1 = \eta_1 D$ and $R_2 = \eta_2 D$. This implies that the sample sizes inhibit the size and shape of incipient dislocations, which further affects the deformation mechanism and yield strength of single crystals. In the light of incipient dislocation plasticity, we focus on the nucleation of the first dislocation in the following discussion.

Figure 7(b) illustrates a schematic image of the dislocation dynamics-based model related to incipient plasticity. If an extended dislocation moves a small distance of Δs, the work done by the dimensional stress τ_D can be written as

$$W_\tau = (R_1 + R_2)\Delta s\phi\tau_D b_p \cos\frac{\pi}{6} = \frac{\sqrt{2}}{4}(\eta_1 + \eta_2)\Delta sD\phi\tau_D a, \tag{3}$$

where a is the lattice length and ϕ is the enclosed angle of curved dislocation. Additionally, the increased SF energy is

$$\Delta E_{\mathrm{SF}} = (R_1 - R_2)\Delta s\phi\gamma_{\mathrm{SF}} = \frac{(\eta_1 - \eta_2)\Delta sD\phi Ga^2}{24\pi d}, \tag{4}$$

where γ_{SF} is the SF energy per unit area [38], G is the shear modulus, and d is the separating distance of two partials in SF. The incremental dislocation line energy (ignoring the core energy of dislocation) is

$$\begin{aligned}\Delta E_d &= \frac{(2-\nu)\Delta s\phi Gb_p^2}{8\pi(1-\nu)}\left(\ln\frac{4R_1}{\rho} + \ln\frac{4R_2}{\rho} - 4\right) \\ &\quad + \frac{(2+\nu)\Delta s\phi Gb_p^2}{8\pi(1-\nu)}\ln\frac{d}{\rho} \\ &= \frac{(2-\nu)\Delta s\phi Ga^2}{48\pi(1-\nu)}\left(\ln\frac{4\eta_1 D}{\rho} + \ln\frac{4\eta_2 D}{\rho} - 4\right) \\ &\quad + \frac{(2+\nu)\Delta s\phi Ga^2}{48\pi(1-\nu)}\ln\frac{d}{\rho},\end{aligned} \tag{5}$$

where the first term denotes the increased self-energy of two partials and the second one describes the increased interaction energy. In (5), ν is Possion's ratio, and ρ is the cutoff radius of a dislocation core and generally, $\rho \cong b_p/8$ [38]. The energy conversation law gives

$$W_\tau = \Delta E_{\mathrm{SF}} + \Delta E_d. \tag{6}$$

By combining (3)–(6) and simplifying, an analytical expression between the dimensional stress τ_D and the sample diameter D is obtained,

$$\begin{aligned}\tau_D &= \frac{\sqrt{2}Ga}{24\pi D(1-\nu)(\eta_1+\eta_2)} \\ &\quad \times \left[(2-\nu)\left(\ln\frac{4\eta_1 D}{\rho} + \ln\frac{4\eta_2 D}{\rho} - 4\right) + (2+\nu)\ln\frac{d}{\rho}\right] \\ &\quad + \frac{\sqrt{2}Ga(\eta_1-\eta_2)}{12\pi d(\eta_1+\eta_2)}.\end{aligned} \tag{7}$$

If the thermal activation stress adds to the analytical dimensional stress, a semi-analytical relation among strength, sample size, temperature, and strain rate is obtained. Under the actual deformation conditions ($\dot{\varepsilon} < 10^{-4}\,\mathrm{s}^{-1}$), the dimensional stress is much greater than the thermal stress. Therefore, this stress-scaling expression can be directly used to estimate the yield strength of microscale single crystals. From the relevant numerical calculations, the following parameters are obtainable directly or indirectly from the present MD simulations:

$$\begin{aligned} &G = 70.97\,\mathrm{GPa}, \quad \nu = 0.312, \quad a = 0.352\,\mathrm{nm}, \\ &d = 3.10\,\mathrm{nm}, \quad \eta_1 = 0.40, \quad \eta_2 = 0.25. \end{aligned} \tag{8}$$

Figure 8 shows the comparison between the dislocation dynamics-based model, experimental, and present MD results. As shown in Figure 8, the dislocation dynamics-based model correlates well with the results from MD simulations, but slightly differs from the experimental datum in the submicron and micron range. One possible reason for this deviation is the neglect of surface effects, such as image forces on dislocations by free surface and influences of surface steps. Although the dislocation dynamics-based model is established on the basis of MD simulations at the nanoscale, this model can be extended to the submicron and micron range because the size effects of single crystals in the nanometer to micron range may be traced to the same physical origin, namely, the dimensional constraint [8]. Indeed, the dislocation density tends to decrease owing to the escape of dislocations from the free surface or dislocation reaction [6, 9], when the micron-scale single crystals are subjected to a nominally uniform compression. Once the dislocation-starved conditions are reached, very high stresses would be required to nucleate new dislocations, either at the surface or in the bulk of the crystal [6]. Thus, the stresses of dislocation nucleation and sudden startup can be estimated by the proposed dislocation dynamic-based model.

The fitting model in Figure 8 shows a stress scaling $\tau \propto D^{-0.69}$ which is different from the usual Hall-Petch relationship $\tau \propto D^{-0.5}$. Power-law exponents close to –0.5 are commonly understood to result from the kinematics of glide obstacles within a linear-glide model, such as grain boundaries [7]. The size effects following a power law with an exponent in the range of $-0.6 \sim -0.7$ arise from influence of both external geometry (such as sample sizes, surface features) and internal structure (such as distribution

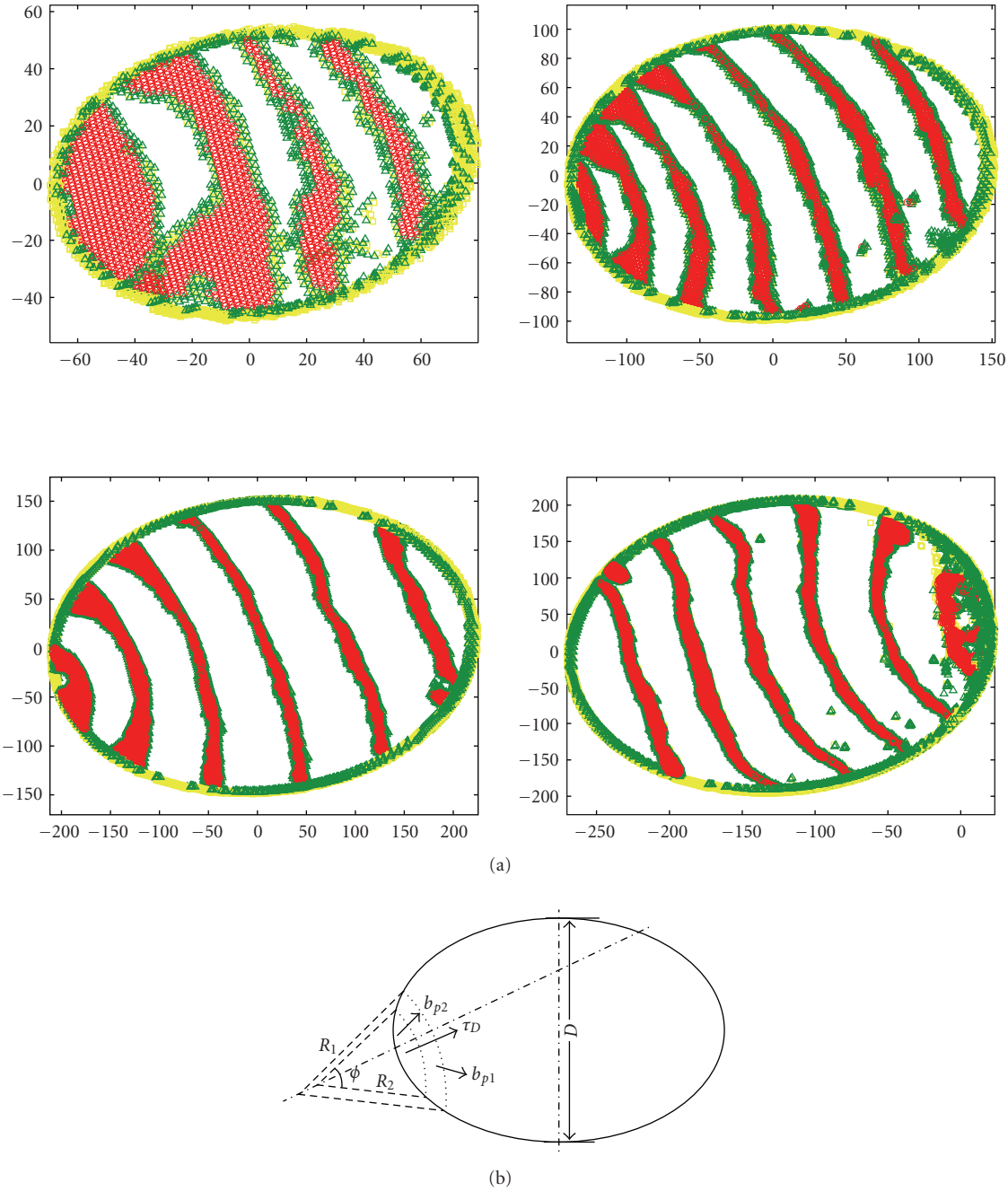

Figure 7: (a) Glide process of the first extended dislocation traveling through the crystal. For nanopillars with different diameters, the configurations of the initial dislocation at different time are placed in a drawing. The drawing plane is the primary slip plane of dislocations. (b) A schematic illustration of dislocation-dynamics-based model.

of dislocation source, obstacle limit) on crystal plasticity. For nanoindentation experiments, plastic deformation is confined within a very small volume, leading to nonuniform stresses and strains which further setup strong gradients of strain [6]. The so-called indentation size effects have been interpreted via strain gradient plasticity models which incorporate the concept of geometrically necessary dislocations. The size effects occurring in the homogenous compression of microscale crystals are associated with dislocation starvation in the absence of stain gradients [6].

The proposed model involves a geometrical assumption that the shape of initially nucleated dislocation is physically limited by the sample sizes. Though it is an observation based on the present MD simulation, it is necessary to verify if this assumption can be experimentally observed via TEM. Notably, the present model predicts only

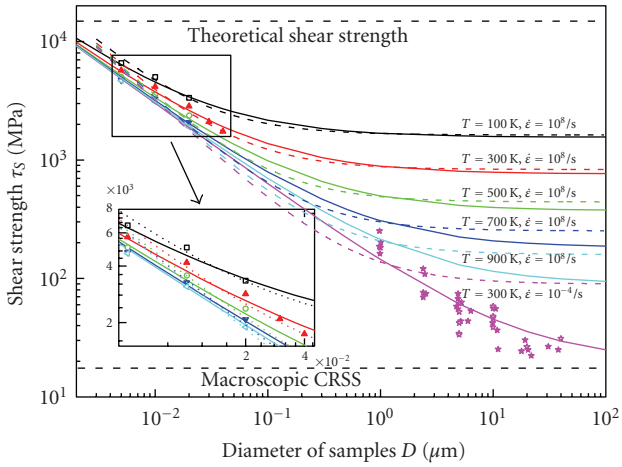

FIGURE 8: Variations of shear yield strengths with sample diameters. Purple-painted star-like data points come from experiments in [5, 7], and other data points come from the present MD simulations. Solid and dashed lines represent the results of the fitting and semi-analytical models, respectively.

the initial stress for crystal plasticity, that is, critical resolved shear stress (CRSS) required for the first percolation of a dislocation across the sample [20]. Since the contributions of image stress to yield strength are neglected, the analytic model is approximate for explaining size effects in the microscale crystals. Nevertheless, this model is available for predicting the yield strength of the single slip-oriented crystal from submicron to micron meters because the image effect gradually diminishes for nucleation and motion of dislocation as the sample size increases.

4. Conclusions

In summary, we show dramatic size dependence of yield strength by performing MD simulations for the compression of Ni single crystals. For single- and octal-slip behaviors, dislocation-mediated plasticity is manifested by dislocation glide, strain bursts, and nanoscale twinning. Both impediment to dislocation motion and formation of nanoscale twins illuminate that sample sizes limit the length scales available for crystal plasticity. Considering sudden nucleation and propagation of the incipient dislocations, we develop a dislocation dynamics-based model whose estimations are in agreement with the results from MD simulations and experiments.

Acknowledgments

This research is sponsored by Grant nos. 10332020 and 10121202 from the National Natural Science Foundation of China, and by Contract no. 2004CB619304 from the 973 Projects of China. The authors are grateful for the supports of parallel computation on HPCS supercomputer at the Chinese Academy of Meteorological Science.

References

[1] S. S. Brenner, "Tensile strength of whiskers," *Journal of Applied Physics*, vol. 27, no. 12, pp. 1484–1491, 1956.

[2] S. S. Brenner, "Plastic deformation of copper and silver whiskers," *Journal of Applied Physics*, vol. 28, no. 9, pp. 1023–1026, 1957.

[3] A. Kelly, *Strong Solids*, Clarendon Press, Oxford, UK, 2nd edition, 1973.

[4] N. A. Fleck, G. M. Muller, M. F. Ashby, and J. W. Hutchinson, "Strain gradient plasticity: theory and experiment," *Acta Metallurgica et Materialia*, vol. 42, no. 2, pp. 475–487, 1994.

[5] M. D. Uchic, D. M. Dimiduk, J. N. Florando, and W. D. Nix, "Sample dimensions influence strength and crystal plasticity," *Science*, vol. 305, no. 5686, pp. 986–989, 2004.

[6] J. R. Greer, W. C. Oliver, and W. D. Nix, "Size dependence of mechanical properties of gold at the micron scale in the absence of strain gradients," *Acta Materialia*, vol. 53, no. 6, pp. 1821–1830, 2005.

[7] D. M. Dimiduk, M. D. Uchic, and T. A. Parthasarathy, "Size-affected single-slip behavior of pure nickel microcrystals," *Acta Materialia*, vol. 53, no. 15, pp. 4065–4077, 2005.

[8] E. Arzt, "Size effects in materials due to microstructural and dimensional constraints: a comparative review," *Acta Materialia*, vol. 46, no. 16, pp. 5611–5626, 1998.

[9] A. A. Benzerga and N. F. Shaver, "Scale dependence of mechanical properties of single crystals under uniform deformation," *Scripta Materialia*, vol. 54, no. 11, pp. 1937–1941, 2006.

[10] V. S. Deshpande, A. Needleman, and E. Van der Giessen, "Plasticity size effects in tension and compression of single crystals," *Journal of the Mechanics and Physics of Solids*, vol. 53, no. 12, pp. 2661–2691, 2005.

[11] H. Tang, K. W. Schwarz, and H. D. Espinosa, "Dislocation escape-related size effects in single-crystal micropillars under uniaxial compression," *Acta Materialia*, vol. 55, no. 5, pp. 1607–1616, 2007.

[12] K. Gall, J. Diao, and M. L. Dunn, "The strength of gold nanowires," *Nano Letters*, vol. 4, no. 12, pp. 2431–2436, 2004.

[13] P. E. Marszalek, W. J. Greenleaf, H. Li, A. F. Oberhauser, and J. M. Fernandez, "Atomic force microscopy captures quantized plastic deformation in gold nanowires," *Proceedings of the National Academy of Sciences of the United States of America*, vol. 97, no. 12, pp. 6282–6286, 2000.

[14] J. Diao, K. Gall, and M. L. Dunn, "Surface-stress-induced phase transformation in metal nanowires," *Nature Materials*, vol. 2, no. 10, pp. 656–660, 2003.

[15] A. Stalder and U. Dürig, "Study of yielding mechanics in nanometer-sized Au contacts," *Applied Physics Letters*, vol. 68, no. 5, pp. 637–639, 1996.

[16] G. Rubio-Bollinger, S. R. Bahn, N. Agraït, K. W. Jacobsen, and S. Vieira, "Mechanical properties and formation mechanisms of a wire of single gold atoms," *Physical Review Letters*, vol. 87, no. 2, Article ID 026101, 4 pages, 2001.

[17] L. Zuo, A. H. W. Ngan, and G. P. Zheng, "Size dependence of incipient dislocation plasticity in Ni_3Al," *Physical Review Letters*, vol. 94, no. 9, Article ID 095501, 4 pages, 2005.

[18] A. H. W. Ngan, L. Zuo, and P. C. Wo, "Size dependence and stochastic nature of yield strength of micron-sized crystals: a case study on Ni_3Al," *Proceedings of the Royal Society A*, vol. 462, no. 2070, pp. 1661–1681, 2006.

[19] L. Zuo and A. H. W. Ngan, "Molecular dynamics study on compressive yield strength in Ni_3Al micro-pillars," *Philosophical Magazine Letters*, vol. 86, no. 6, pp. 355–365, 2006.

[20] T. A. Parthasarathy, S. I. Rao, D. M. Dimiduk, M. D. Uchic, and D. R. Trinkle, "Contribution to size effect of yield strength from the stochastics of dislocation source lengths in finite samples," *Scripta Materialia*, vol. 56, no. 4, pp. 313–316, 2007.

[21] Z. W. Shan, R. K. Mishra, S. A. Syed Asif, O. L. Warren, and A. M. Minor, "Mechanical annealing and source-limited deformation in submicrometre-diameter Ni crystals," *Nature Materials*, vol. 7, no. 2, pp. 115–119, 2008.

[22] Y. Mishin, D. Farkas, M. J. Mehl, and D. A. Papaconstantopoulos, "Interatomic potentials for monoatomic metals from experimental data and ab initio calculations," *Physical Review B*, vol. 59, no. 5, pp. 3393–3407, 1999.

[23] M. Tuckerman, B. J. Berne, and G. J. Martyna, "Reversible multiple time scale molecular dynamics," *The Journal of Chemical Physics*, vol. 97, no. 3, pp. 1990–2001, 1992.

[24] W. G. Hoover, *Computational Statistical Mechanics*, Elsevier, New York, NY, USA, 1991.

[25] J. D. Honeycutt and H. C. Andersen, "Molecular dynamics study of melting and freezing of small Lennard-Jones clusters," *Journal of Physical Chemistry*, vol. 91, no. 19, pp. 4950–4963, 1987.

[26] H. Van Swygenhoven, D. Farkas, and A. Caro, "Grain-boundary structures in polycrystalline metals at the nanoscale," *Physical Review B*, vol. 62, no. 2, pp. 831–838, 2000.

[27] X.-L. Ma and W. Yang, "Molecular dynamics simulation on burst and arrest of stacking faults in nanocrystalline Cu under nanoindentation," *Nanotechnology*, vol. 14, no. 11, pp. 1208–1215, 2003.

[28] D. Wolf, V. Yamakov, S. R. Phillpot, A. Mukherjee, and H. Gleiter, "Deformation of nanocrystalline materials by molecular-dynamics simulation: relationship to experiments?" *Acta Materialia*, vol. 53, no. 1, pp. 1–40, 2005.

[29] S. J. A. Koh, H. P. Lee, C. Lu, and Q. H. Cheng, "Molecular dynamics simulation of a solid platinum nanowire under uniaxial tensile strain: temperature and strain-rate effects," *Physical Review B*, vol. 72, no. 8, Article ID 085414, 11 pages, 2005.

[30] M. F. Horstemeyer, M. I. Baskes, and S. J. Plimpton, "Length scale and time scale effects on the plastic flow of fcc metals," *Acta Materialia*, vol. 49, no. 20, pp. 4363–4374, 2001.

[31] T. Zhu, J. Li, A. Samanta, A. Leach, and K. Gall, "Temperature and strain-rate dependence of surface dislocation nucleation," *Physical Review Letters*, vol. 100, no. 2, Article ID 025502, 4 pages, 2008.

[32] C. A. Schuh and A. C. Lund, "Application of nucleation theory to the rate dependence of incipient plasticity during nanoindentation," *Journal of Materials Research*, vol. 19, no. 7, pp. 2152–2158, 2004.

[33] P. C. Wo, L. Zuo, and A. H. W. Ngan, "Time-dependent incipient plasticity in Ni_3Al as observed in nanoindentation," *Journal of Materials Research*, vol. 20, no. 2, pp. 489–495, 2005.

[34] M. Dao, L. Lu, Y. F. Shen, and S. Suresh, "Strength, strain-rate sensitivity and ductility of copper with nanoscale twins," *Acta Materialia*, vol. 54, no. 20, pp. 5421–5432, 2006.

[35] F. J. Zerilli and R. W. Armstrong, "Dislocation-mechanics-based constitutive relations for material dynamics calculations," *Journal of Applied Physics*, vol. 61, no. 5, pp. 1816–1825, 1987.

[36] F. J. Zerilli and R. W. Armstrong, "Description of tantalum deformation behavior by dislocation mechanics based constitutive relations," *Journal of Applied Physics*, vol. 68, no. 4, pp. 1580–1591, 1990.

[37] J. Gil Sevillano, I. Ocaña Arizcorreta, and L. P. Kubin, "Instrinsic size effects in plasticity by dislocation glide," *Materials Science and Engineering A*, vol. 309-310, pp. 393–405, 2001.

[38] J. P. Hirth and J. Lothe, *Theory of Dislocations*, McGraw-Hill, New York, NY, USA, 1st edition, 1968.